


# TRIB3 Is a Hub Gene in Steatohepatitis and Aggravates Lipid Deposition and Inflammation in Hepatocytes

Wen Xia<sup>1,\*</sup>, Li Xiao<sup>1,\*</sup>, Huan Cheng<sup>1</sup>, Yuwei Feng<sup>2</sup> 

<sup>1</sup>Department of Cardiovascular Medicine, Wuhan No.1 Hospital, Wuhan, Hubei, People's Republic of China; <sup>2</sup>Department of Hepatology with Integrated Traditional Chinese and Western Medicine, Hubei No.3 People's Hospital of Jiangnan University, Wuhan, Hubei, People's Republic of China

\*These authors contributed equally to this work

Correspondence: Yuwei Feng, Department of Hepatology with Integrated Traditional Chinese and Western Medicine, Hubei No.3 People's Hospital of Jiangnan University, #26 Zhongshan Avenue, Wuhan, 430022, People's Republic of China, Tel +86-27-85332356, Email fengyw92@163.com

**Background:** Non-alcoholic fatty liver disease (NAFLD), also known as Metabolic dysfunction-associated fatty liver disease (MASLD), has become one of the most common chronic liver diseases worldwide, approximately 30% of adults and 70%–80% of patients with obesity and diabetes suffer from NAFLD.

**Objective:** We attempted to find a potential hub gene in NAFLD hepatocyte cell model induced by palmitic acid and oil acid (PAOA), and investigated the function of the hub-gene.

**Methods:** We searched and downloaded the GSE122660 dataset from GEO-Datasets, and differentially expressed genes (DEGs) were analyzed using R software. Gene Ontology (GO) and Kyoto Encyclopedia of Genes and Genomes (KEGG) pathway enrichment analyses were performed to identify the significantly activated signaling pathways in steatohepatitis. A protein-protein interaction (PPI) network was constructed to identify hub genes among the DEGs. qRT-PCR, Western blotting, and Oil Red O staining were used to explore the function of hub genes in PAOA-induced hepatocytes in vitro.

**Results:** A total of 255 DEGs were identified in the GSE122660 dataset and were primarily associated with inflammation and lipid metabolism-related pathways. The tribbles pseudokinase 3 (TRIB3) was highlighted as a hub gene. We found that TRIB3 was upregulated in CDHFD-induced NAFLD mouse liver tissue and hepatocyte cell models. Furthermore, TRIB3 aggravated PAOA-induced lipid accumulation and inflammation in hepatocytes in vitro.

**Conclusion:** The present study identified TRIB3 as a hub gene for steatohepatitis and aggravated lipid accumulation and inflammation in vitro. Therefore, targeting TRIB3 could be a potential pharmacological strategy for NAFLD treatment.

**Keywords:** non-alcoholic fatty liver disease, steatohepatitis, hub gene, TRIB3, lipid accumulation, inflammation

## Introduction

Non-alcoholic fatty liver disease (NAFLD), also known as metabolic dysfunction-associated fatty liver disease (MASLD) now, has emerged as a major cause of chronic liver disease in both children and adults worldwide with an estimated global prevalence of 25.2% (range 22.1–28.6%).<sup>1,2</sup> Approximately a quarter of adults with NAFLD are projected to develop non-alcoholic steatohepatitis (NASH), a dynamic condition that can regress to isolated steatosis based on elevated serum aminotransferase levels and the absence of other competing liver injuries, with an estimated global prevalence of NASH in NAFLD biopsy patients is 59.1%.<sup>3</sup> Etiologically, multiple conditions, including age, genetics, innate immunity, and metabolic syndrome (MetS), lead to NASH, which typically includes obesity, insulin resistance, hyperglycemia, and dyslipidemia.<sup>4</sup> Clinically, NASH is strongly associated with cardiovascular diseases (CVDs),<sup>5</sup> and up to one-third of patients with NASH have increased liver-related mortality, attributed to progression to advanced fibrosis or cirrhosis and hepatocellular carcinoma

(HCC).<sup>6</sup> However, no effective NASH-specific pharmacological strategies have been approved by the FDA.<sup>7</sup> Therefore, the mechanisms underlying NAFLD require further investigation.

Tribbles pseudokinase 3 (*TRIB3*) is a member of the tribble-related family, which contains a Ser/Thr protein kinase-like domain but lacks a 5'-adenosine triphosphate-binding pocket and catalytic core motifs.<sup>8</sup> Numerous studies have indicated that *TRIB3* plays a crucial role in various cellular processes including cell proliferation and differentiation, epithelial-to-mesenchymal transition, cellular stress response, and glucose and glucolipid metabolism.<sup>9–11</sup> This involvement is achieved through its interaction with several transcriptional mediators such as CCAAT-enhancer-binding protein homologous protein (*CHOP*), peroxisome proliferator-activated receptor alpha (*PPARα*), and activating transcription factor 4 (*ATF4*).<sup>12,13</sup> Previously, *TRIB3* has been demonstrated to be closely related to tumor processes, including non-small-cell lung cancer,<sup>14</sup> glioma,<sup>15</sup> breast cancer,<sup>16</sup> oral squamous cell carcinoma,<sup>17</sup> hepatocellular carcinoma<sup>18</sup> and colorectal cancer.<sup>19</sup> Recent studies have shown that *TRIB3* plays an important role in metabolic disorders. Lee et al revealed that *TRIB3* expression is increased in the adipose tissue of obese patients, indicating that increased *TRIB3* dysregulates adipocyte function, which contributes to the development of insulin resistance.<sup>20</sup> Prudente et al reviewed the role of *TRIB3* in glucose homeostasis and showed that *TRIB3* overexpression was observed in the liver, adipose tissue, skeletal muscle, and pancreatic β-cells of individuals with insulin resistance and/or T2DM.<sup>9</sup> *TRIB3* overexpression or gain-of-function variant (*TRIB3* Q84R) is involved in insulin resistance, T2DM, and cardiovascular disease.<sup>9</sup> Particularly, *TRIB3* is markedly increased in liver tissue in animal models of insulin resistance, obesity, hyperglycemia.<sup>12,21,22</sup> However, the role of *TRIB3* in NAFLD remains to be elucidated.

In the present study, we downloaded and analyzed the gene expression profiles of Huh7 hepatocytes induced by palmitic acid and oleic acid (PAOA), which was identified as a cell model of NAFLD. Differentially expressed genes (DEGs) were identified in these samples. Gene Ontology (GO) and Kyoto Encyclopedia of Genes and Genomes (KEGG) pathway functional enrichment analyses were performed using DEGs to reveal the key pathways. Protein-protein interaction (PPI) network analysis was used to identify potential hub genes in PAOA-induced hepatocytes, and *TRIB3* was highlighted among the top 20 hub genes. Finally, we validated the expression and revealed the function of *TRIB3* in PAOA induced hepatocytes. Our data suggest that *TRIB3* is a potential therapeutic target for the treatment of NAFLD.

## Methods

### Data Sources

The GSE122660 dataset was obtained from the Gene Expression Omnibus (GEO) database (<http://www.ncbi.nlm.nih.gov/geo/>). Six samples of Huh7 cells were included in the GSE122660 dataset, including three samples treated with DMSO as a control and three samples treated with Palmitic Acid and Oleic Acid (PAOA) for the steatohepatitis models. The GPL13158 platform was used to sequence the GSE122660 sequencing.

### DEGs Analysis

UMAP and volcano plots were analyzed and constructed using GEO2R (<https://www.ncbi.nlm.nih.gov/geo/geo2r>). The gene expression profiling analysis were preprocessed by a R software (version 4.4.1, 82 megabytes, 64 bit, R Foundation for Statistical Computing, Vienna, Austria) with “affy” and “affyPLM” packages. We processed the raw data of these datasets using the R package “limma” for background correction and data normalization.

The DEGs were screened with an adjusted p-value <0.05 and |logFC >1|. A heatmap analysis was performed using ImageGP (<http://www.ehbio.com>).

### Gene Ontology and Kyoto Encyclopedia of Genes and Genomes

The Gene Ontology (GO) and Kyoto Encyclopedia of Genes and Genomes (KEGG) analysis for the DEGs were performed by Database for Annotation, Visualization and Integrated Discovery (DAVID, <http://david.ncifcrf.gov>), the plots were drawn by ImageGP.

## PPI Construction and Hub Genes Screening

The STRING database (<https://string-db.org/>) was used to identify possible protein–protein interaction network interactions (PPI interaction score > 0.4). The PPI network was constructed using the Cytoscape software platform (version 3.9.0) and the top 20 hub genes were identified using the CytoHubba plugin.

## Mice Feeding and Histopathology Analysis

All mice were raised at the Laboratory Animal Center of Huazhong University of Science and Technology. All animal experiments were reviewed and approved by the Animal Experimentation Ethics Committee of Huazhong University of Science and Technology ([2023] IACUC #6022). All procedures were conducted in accordance with the guidelines of the Institutional Animal Care and Use Committee of Huazhong University of Science and Technology.

Sixteen 6-week male mice were randomly divided into the NASH group and control group. The animal model of NASH was established by feeding a choline-deficient high-fat diet (CDHFD, caloric distribution: 18% from protein, 62% from fat, and 20% from carbohydrates; SYSE BIO, Suzhou, China) for 8 weeks. Mice fed with a normal chow diet (NC, caloric distribution: 20.6% from protein, 12.0% from fat and 67.4% from carbohydrates; SYSE BIO, Suzhou, China) were used as controls. The composition and content of CDHFD diet was listed in [Supplementary Table 1](#).

Liver samples were embedded in paraffin, then the embedded liver tissue was sectioned to a thickness of 5  $\mu$ m. Sections were loaded onto slides and deparaffinized for hematoxylin and eosin (H&E) staining to analyze lipid accumulation. OCT-embedded frozen liver tissues were used for Oil Red O staining and the thickness of the sections was 5  $\mu$ m. The histological features of the tissues were observed and imaged using a light microscope.

Primary hepatocytes were isolated from eight-week-old C57BL/6J male mice. Briefly, mice were perfused after anesthetization and perfused with 0.05% type IV collagenase. Then, the primary hepatocytes were obtained after liver was excised, minced and filtered. The obtained hepatocytes were resuspended in DMEM and seeded in plates. The adenovirus loading the Trib3 gene (Ad-Trib3-Flag) and empty vector (Ad-Flag) were purchased from GENECHM (Shanghai, China).

## Cells and Treatment

The human hepatocyte cell line L02 was purchased from the Type Culture Collection of the Chinese Academy of Sciences (Beijing, China). Cells were cultured in DMEM (Invitrogen, Carlsbad, CA, USA) supplemented with 10% FBS under 5% CO<sub>2</sub> at 37 °C. The cells were seeded in six-well plates at a density of 2×10<sup>5</sup> cells/well. 0.5mM palmitic acid and 1 mm oil acid (PAOA) were used to establish an in vitro model of NAFLD in L02 cells. The cells were fixed with 4% paraformaldehyde for 20 min and stained with a 60% Oil Red O working solution for one minute to induce intracellular lipid accumulation.

## Plasmid Construction

The human TRIB3 consensus CDS region was cloned into pHAGE-Flag to construct the EGR2 expression vector pHAGE-Flag-TRIB3. The empty vector pHAGE-Flag was used as the control plasmid. Primer sequences: forward, 5'-ATGCGAGCCACCCCTCTGGC-3'; Reverse: 5'-GCCATACAGAACCACTTCTC-3.

## siRNA Transfection

The sham siRNA and siTRIB3 (siTRIB3-1 and siTRIB3-2), designed and synthesized by RiboBio (Guangzhou, China), were transfected at 50nM using Lipofectamine R\_2000 reagent (Invitrogen), following the manufacturer's protocol. The siRNA target sequences were as follows: sham siRNA (control), 5'-GTGTTTGATGACCCGTTTA-3; siTRIB3-1, 5'-TGGGATTTGGGCCAGAGATAAGA-3; siTRIB3-2, 5'-GTCCATACTCTAGGTTTTGGATA-3.

## RT-qPCR

Total RNA was extracted using TRIzol reagent and converted to cDNA using HiScript II Q RT SuperMix for qPCR (+gDNA wiper) (Vazyme, China). qPCR was conducted using the ChamQ SYBR qPCR Master Mix (Vazyme, China). The data were calculated the SDS 2.2.1 software. The primers used are listed in [Table 1](#).

**Table 1** Primers of RT-qPCR Assays

Gene Symbol	Forward (5' to 3')	Forward (5' to 3')
TRIB3	AAGCGTTGGAGTTGGATGAC	CACGATCTGGAGCAGTAGGTG
CD36	AAGCCAGGTATTGCAGTTCTTT	GCATTTGCTGATGTCTAGCACA
FASN	AAGGACCTGTCTAGGTTTGATGC	TGGCTTCATAGGTGACTTCCA
SREBP1c	ACAGTGACTTCCCTGGCCTAT	GCATGGACGGGTACATCTTCAA
SCD1	TCTAGCTCCTATACCACCACCA	TCGTCTCCAATTATCTCCTCC
IL6	ACTCACCTCTTCAGAACGAATTG	CCATCTTTGGAAGGTTCAAGTTG
IL1b	ATGATGGCTTATTACAGTGGCAA	GTCGGAGATTCGTAGCTGGA
CCL2	CAGCCAGATGCAATCAATGCC	TGGAATCCTGAACCCACTTCT
CXCL12	ATTCTCAACACTCCAACTGTGC	ACTTTAGCTTCGGGTCAATGC
β-ACTIN	CATGTACGTTGCTATCCAGGC	CTCCTTAATGTCACGCACGAT

## Western Blot

For Western blot analysis, total protein was isolated from cells and liver tissue using RIPA lysis buffer, and its concentration was determined using a BCA Protein Assay Kit (#AR1189, BOSTER). Protein samples were separated using 10% SDS-PAGE, transferred to PVDF membranes, and blocked with 5% skim milk. The membranes were then incubated with primary and secondary antibodies. Images were obtained using a ChemiDoc MP Imaging System (Bio-Rad, Hercules, CA, USA). Antibodies: anti-TRIB3, #13300-1-AP, Proteintech; anti-β-actin, #81115-1-RR, Proteintech; anti-FLAG, #20543-1-AP, Proteintech; and Multi-rAb HRP-Goat Anti-Rabbit Recombinant Secondary Antibody (H+L), # GAR001, Proteintech.

## Statistical Analysis

All data are presented as mean ± standard deviation (SD) of three independent experiments using Prism 9. Significance was assessed using one-way ANOVA followed by Tukey's test. All statistical analyses were performed using SPSS 22.1 (SPSS Inc., Chicago, IL, USA). Statistical significance was set at p value < 0.05.

## Results

### Bioinformation Analysis from the GSE122660 Dataset and Identification of DEGs

To investigate the expression of the transcriptome in hepatocytes under steatohepatitis conditions, we selected and downloaded the GSE122660 dataset from the GEO DataSets. The design of the data analysis process is illustrated in the flow diagram (Figure 1A). Briefly, the GSE122660 dataset was preprocessed using R software, and DEGs were identified. GO and KEGG pathway analyses were performed to reveal the key pathways, and hub genes were identified by PPI network analysis. Finally, hub gene function in steatohepatitis was validated in vitro. UMAP analysis showed that six samples were clustered into the PAOA and DMSO control groups (Figure 1B), indicating that the genomic expression in PAOA-induced hepatocytes was significantly different from that in control cells. A volcano plot showed differentially expressed genes in PAOA-induced Huh7 and control cells (p < 0.05) (Figure 1C). In addition, heatmap analysis revealed 255 differentially expressed genes (DEGs) that met the adjusted p value < 0.05 and |logFC| > 1, including 117 downregulated and 138 upregulated genes (Figure 1D). The top 20 upregulated and downregulated DEGs are listed in Table 2, most of which were related to lipid metabolism and inflammation, including lysosome-associated membrane protein 3 (*LAMP3*), Kruppel-like factor 4 (*KLF4*), solute carrier family 3 member 2 (*SLC3A2*), and DNA damage-inducible transcript 3 (*DDIT3*).

### Functional Enrichment Analyses of DEGs

To further understand the function of EDGs in PAOA-induced hepatocytes, GO and KEGG comprehensive analyses of the functions of these DEGs were performed. In GO enrichment analysis, 81 GO terms were enriched (p < 0.05), including 47 biological processes (BP), 16 cellular components (CC), and 18 molecular function (MF) terms. For BP, the



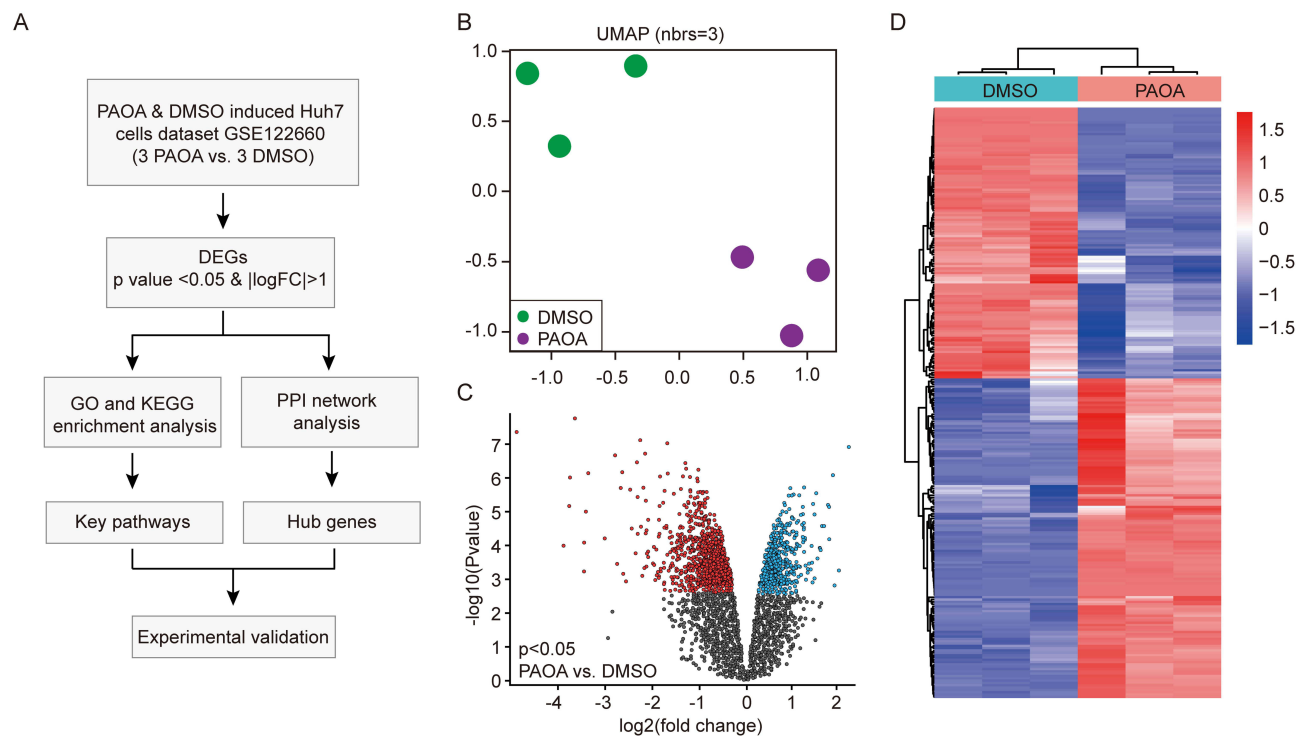


**Figure 1** Differentially expressed genes in Huh7 cells induced by PAOA compared to control cells. **(A)** The flow diagram for the analysis procedure of this present study. **(B)** UMAP plot was used to visualize the relationships between PAOA induced cells and control cells, purple dots represent the PAOA induced cell samples and the green dots represent the control samples. **(C)** Volcano plot of p values as a function of the weighted p value for genes in PAOA induced Huh7 cells and control cells. Gray dots represent genes that are not significantly differentially expressed ( $p > 0.05$ ), red dots represented the genes that are significantly upregulated in Huh7 cells with PAOA stimulation ( $p < 0.05$ ), the baby blue dots represent the genes that are significantly downregulated in PAOA group samples ( $p < 0.05$ ). **(D)** Heatmap shows the expression profiles for the 255 differentially expressed genes (117 downregulated and 138 upregulated). The red to green color gradient indicates a high to low level of expression.  $p < 0.05$ ,  $|\logFC| > 1$ . For B to D,  $n = 3$  samples in each group.

DEGs were mostly enriched in inflammation-, apoptosis-, and lipid-metabolism-related terms (Figure 2A), including response to endoplasmic reticulum stress, response to unfolded protein, endoplasmic reticulum unfolded protein response, intrinsic apoptotic signaling pathway in response to endoplasmic reticulum stress, chemokine-mediated signaling pathway, positive regulation of the apoptotic process, regulation of autophagy, lipoprotein metabolic process,

**Table 2** The Top 20 Upregulated and Downregulated Genes of DEGs

Gene Symbol	LogFC	P value	Gene Symbol	LogFC	P value
LAMP3	4.07	0.00	PITX2	-2.28	0.00
FAM129A	3.49	0.00	CCR6	-2.28	0.00
INHBE	2.69	0.00	CFHR5	-2.11	0.00
PARM1	2.68	0.00	SLC23A1	-2.03	0.00
SLC3A2	2.65	0.00	CLRN3	-1.95	0.00
KLF4	2.57	0.00	RBP2	-1.92	0.00
SOCS2	2.55	0.00	ALDH8A1	-1.87	0.00
RAB39B	2.48	0.00	CDH17	-1.72	0.02
SI00P	2.41	0.00	ADH6	-1.69	0.00
ZNF165	2.38	0.00	HPR	-1.68	0.00
FBXO16	2.38	0.00	LGALS2	-1.68	0.01
TMEM140	2.33	0.00	NTS	-1.65	0.02
KCNK6	2.32	0.00	TFF2	-1.62	0.00

(Continued)

**Table 2** (Continued).

Gene Symbol	LogFC	P value	Gene Symbol	LogFC	P value
SLC22A15	2.16	0.00	GBA3	−1.59	0.00
PLA1A	2.13	0.01	CXCL10	−1.59	0.00
CYP24A1	2.11	0.00	NAT8B	−1.58	0.00
FIBIN	2.10	0.00	HIST1H2BC	−1.56	0.01
EREG	2.06	0.00	C6orf142	−1.53	0.00
PPP1R15A	2.03	0.00	HIST1H2AL	−1.52	0.00
DDIT3	1.98	0.00	LOC100128191	−1.50	0.00

long-chain fatty acid metabolic process. Regarding CC, the endoplasmic reticulum lumen, endoplasmic reticulum membrane, extracellular region, extracellular exosome, extracellular space, and perinuclear region of the cytoplasm were enriched (Figure 2B). In MF, DEGs were mostly enriched in sequence-specific double-stranded DNA binding, RNA polymerase II transcription factor activity, sequence-specific DNA binding, protein binding, transcriptional repressor activity, RNA polymerase II transcription regulatory region sequence-specific binding, and transcription regulatory region sequence-specific DNA binding terms (Figure 2C). In the KEGG pathway enrichment analysis, the DEGs were most significantly enriched in 10 pathways related to inflammation, lipid metabolism, and cell apoptosis (Figure 2D), including tryptophan metabolism, complement and coagulation cascades, apoptosis, the MAPK signaling pathway, fatty acid degradation, and alanine aspartate and glutamate metabolism.

## Protein–Protein Interaction Network Construction and Hub Gene Identification

To reveal the association between the 255 DEGs, we constructed a PPI network and evaluated their interactions using the STRING database. After STRING database calculation, 147 nodes and 324 connections were generated, and the PPI was visualized using Cytoscape software (Figure 3A). Importantly, the top 20 DEGs with a high degree of connectivity were selected as hub genes in the PAOA-stimulated hepatocytes (Figure 3B and Table 3). Most hub genes are related to inflammation and have been reported to play roles in inflammation and NAFLD, such as AP-1 transcription factor subunit (*JUN*), *DDIT3*, very low-density lipoprotein receptor (*VLDLR*), eukaryotic translation initiation factor 2 alpha kinase 3 (*EIF2AK3*), and *TRIB3*. However, the function of the hub gene *TRIB3* in steatohepatitis remains unclear.

## TRIB3 Is up-Regulated in NASH Model in vivo and in vitro

To investigate the function of *TRIB3* in steatohepatitis, we first established a mouse NASH model and steatohepatitis cell model, then detected the expression of *TRIB3* under NASH conditions in vivo and in vitro. H&E and ORO staining showed that after eight weeks of CDHFD induction, hepatocellular ballooning and lipid accumulation developed significantly in the mouse liver (Figure 4A). We detected the expression of *Trib3*-mRNA and -protein levels in mouse livers induced by NC or CDHFD using qPCR and Western blot assays. Our results showed that *Trib3* was upregulated at the mRNA and protein levels in CDHFD-induced mouse livers compared to those in the NC group (Figure 4B and C). In vitro, we established a NASH cell model using a human hepatocyte cell line and mouse primary hepatocytes stimulated with PAOA, and BSA-treated cells were used as a control (Figure 4D and G). Using hepatocyte cell line and mouse primary hepatocytes, we examined the mRNA and protein expression levels of *TRIB3* in PAOA-induced hepatocyte and control cells by qRT-PCR and Western blot assays, and found that *TRIB3* was markedly upregulated in the steatohepatitis cell model (Figure 4E, F, H and I). Taken together, these data suggest that *TRIB3* is activated in both in vivo and in vitro NASH models.

## TRIB3 Overexpression Aggravates PAOA-Induced Lipid Accumulation and Inflammation in Hepatocytes

We overexpressed *TRIB3* in hepatocytes by pHAGE-Flag-*TRIB3* plasmid transfection, and the expression level of *TRIB3* was confirmed by qRT-PCR and Western blotting (Figure 5A and B). As expected, 24 h after PAOA stimulation, the Oil Red O assay

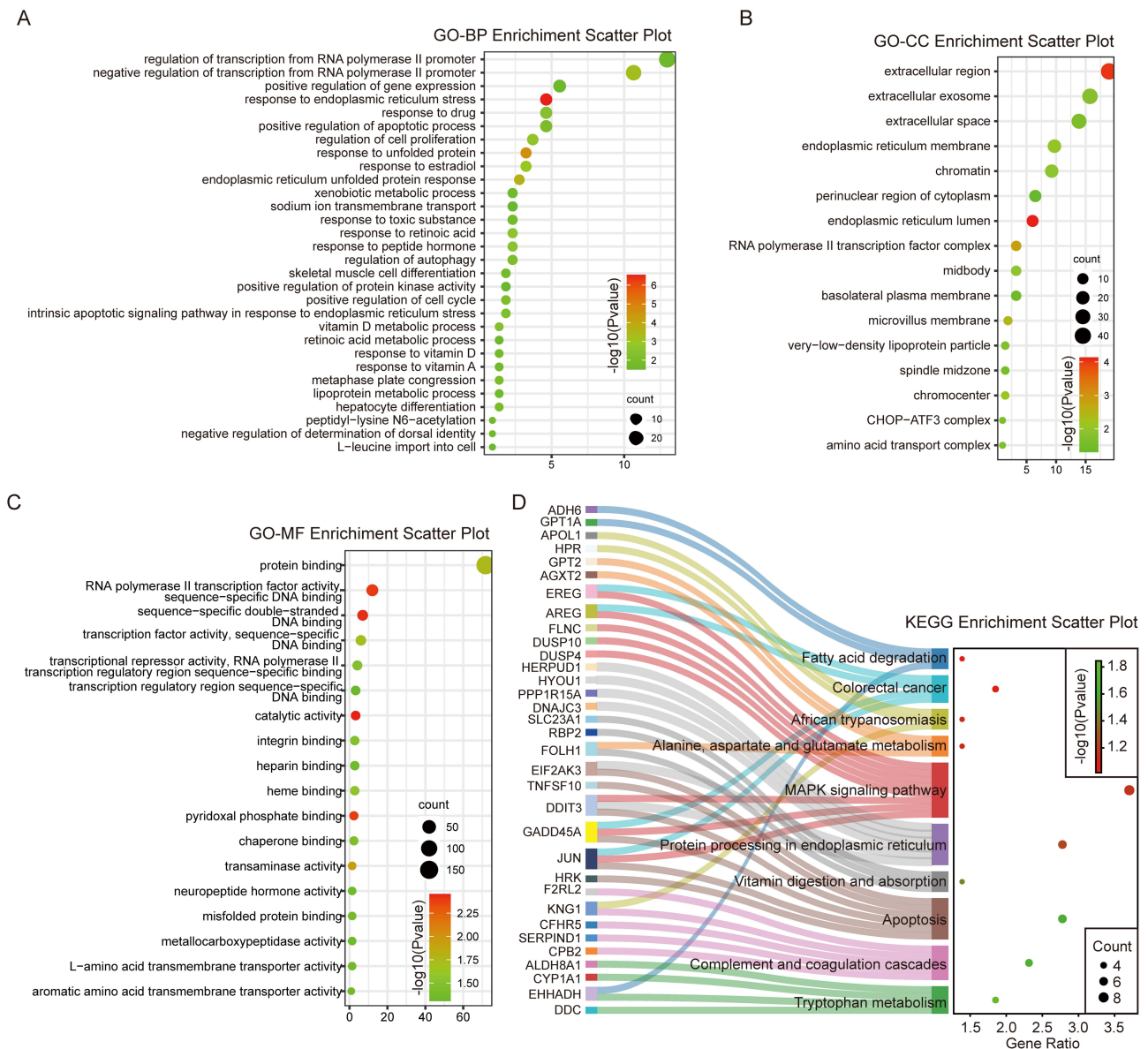


**Figure 2** Gene ontology (GO) and Kyoto Encyclopedia of Genes and Genome (KEGG) enrichment analysis. **(A)** The top 30 significant GO biological process terms. **(B)** the most significant GO molecular function terms. **(C)** The significant GO cellular component terms. **(D)** The enriched KEGG pathway terms. The circle size of the dots represents gene counts in each enriched term. The different color means significance for each enriched term.

revealed a significant increase in lipid deposition in TRIB3-overexpressed hepatocytes compared to that in control cells (Figure 5C). We further established Trib3-overexpressing mouse primary hepatocytes by transfected with an adenovirus vector loading the Trib3 gene (Ad-Trib3-Flag), the Ad-Flag was used as control (Figure 5D). 24 h after PAOA treatment, compared with Ad-Flag controls, the Oil Red O staining showed the lipid accumulation in Trib3 overexpressed mouse primary hepatocytes (Figure 5E). To further evaluate the function of TRIB3 overexpression in steatohepatitis, we examined the expression of inflammatory, lipid uptake-, and lipid synthesis-related genes in PAOA-induced hepatocytes. Our results showed that TRIB3 overexpression remarkably increased the expression of lipid uptake and synthesis genes, including CD36, FASN, SCD1, and SREBP1c (Figure 5F). Additionally, the expression of proinflammatory genes (IL-6, IL-1b, CCL2, and CCL12) expression in TRIB3 overexpressed hepatocytes was significantly activated by PAOA stimulation (Figure 5G). Collectively, these data suggested that excessive TRIB3 exacerbates lipid accumulation and inflammatory responses in hepatocytes during steatohepatitis.

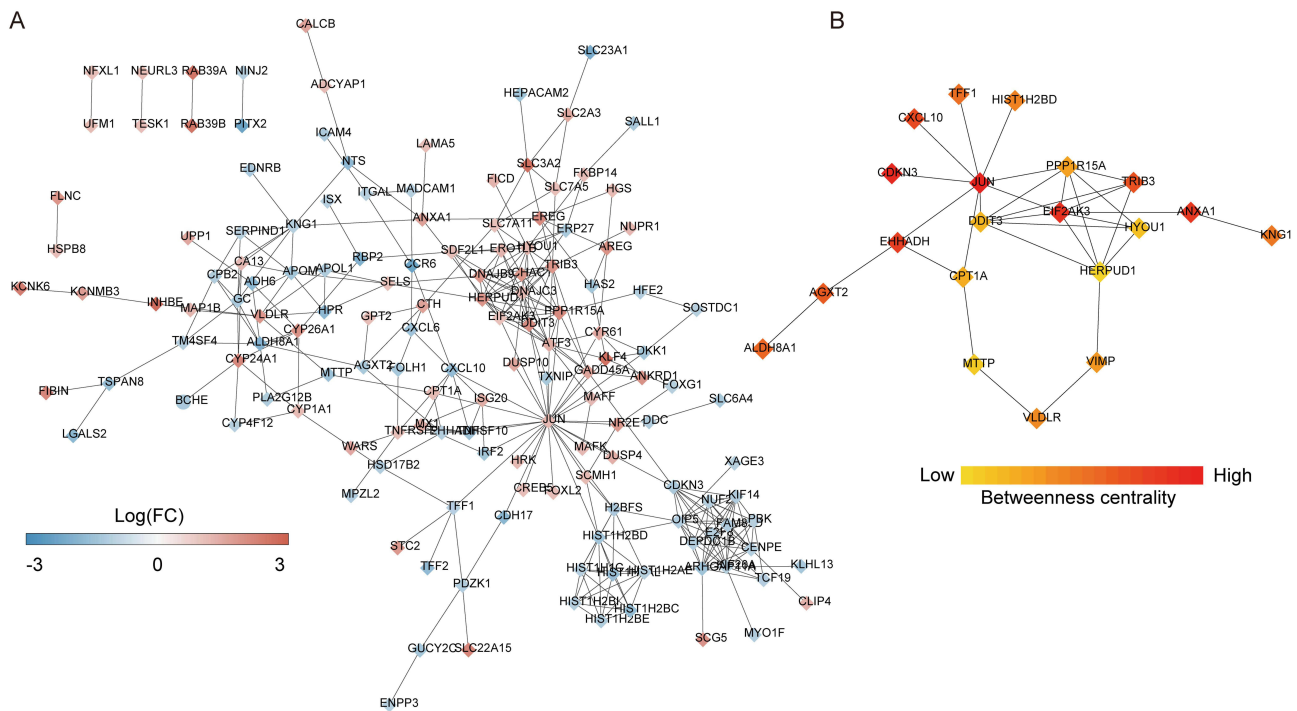


**Figure 3** Protein–protein interaction (PPI) networks and hub genes of differential expressed genes in PAOA induced Huh7 cells compared with control cells. **(A)** PPI networks show the interaction of differential expressed genes in PAOA treated cells and control cells. The red to blue color gradient indicates an upregulation to downregulation of differential expressed genes which indicated by logFC. **(B)** The top 20 hub genes from differential expressed gene. The red to yellow color gradient indicates a high to low centrality.

### Inhibition the Expression of TRIB3 Ameliorates PAOA–Induced Lipid Accumulation and Inflammation in Hepatocytes

To reveal the function of TRIB3-loss in steatohepatitis, we established TRIB3-knockdown hepatocytes by siRNA transfection. qPCR showed that TRIB3 expression was significantly suppressed by siTRIB3-1 and siTRIB3-2 (Figure 6A). After 24h of PAOA stimulation, Oil Red O staining showed improved lipid accumulation in hepatocytes transfected with siTRIB3-1 and siTRIB3-2 compared with that in hepatocytes transfected with sham siRNA (Figure 6B). Moreover, qPCR showed that the downregulation of TRIB3 remarkably decreased the expression of lipid uptake genes (CD36) and synthesis genes (FASN, SCD1, and SREBP1c) in PAOA-induced hepatocytes (Figure 6C). PAOA-induced inflammation in hepatocytes was significantly alleviated after TRIB3 knockdown, as indicated by the mRNA expression

**Table 3** The Hub Genes of DEGs

Gene Symbol	LogFC	P value	Connectivity Score	Gene Symbol	LogFC	P value	Connectivity Score
JUN	1.13	0.00	11,161.17	KNG1	-1.03	0.01	1245.78
CDKN3	-1.22	0.01	3306.87	HIST1H2BD	-1.33	0.00	1214.76
EIF2AK3	1.01	0.00	2471.94	VLDLR	1.82	0.00	1155.50
ANXA1	1.62	0.01	2035.02	CPT1A	1.14	0.00	1116.11
EHHADH	-1.07	0.01	1842.91	PPP1R15A	2.03	0.00	1075.32
CXCL10	-1.59	0.00	1839.36	MTTP	-1.43	0.02	1003.67
TRIB3	1.83	0.00	1710.07	DDIT3	1.98	0.00	1000.77
AGXT2	-1.23	0.00	1661.30	SELS	1.02	0.01	982.16
ALDH8A1	-1.87	0.00	1621.82	HYOU1	1.21	0.00	950.07
TFF1	-1.04	0.01	1505.68	GADD45A	1.56	0.00	879.55



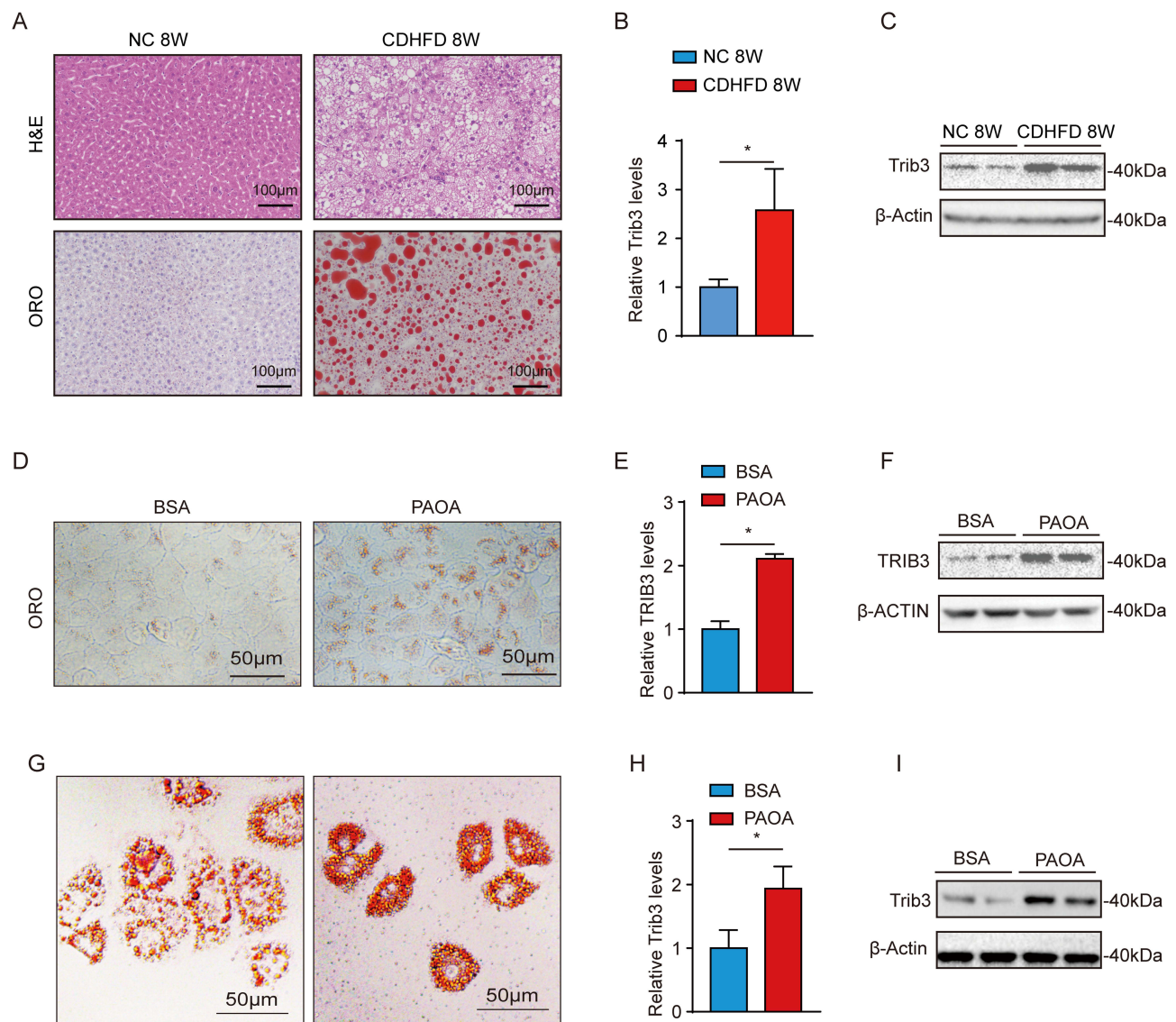


**Figure 4** TRIB3 is up-regulated in NASH model in vivo and in vitro. **(A)** Representative H&E- and ORO-staining images of mouse liver induced by CDHFD and NC for 8 weeks, scale bar = 100μm, n = 7 mice per group. **(B)** The mRNA levels of Trib3 in mouse livers from CDHFD and NC groups, β-Actin was used as internal control, n = 4 per group. **(C)** Western blot assay showed the Trib3 protein levels in mouse livers from indicated groups, β-Actin was used as internal control. **(D)** Representative ORO-staining images of hepatocytes simulated by PAOA/BSA for 24 hours, scale bar = 50μm. **(E)** The mRNA levels of TRIB3 in PAOA/BSA-treated human hepatocytes, β-ACTIN was used as internal control, n = 3 per group. **(F)** TRIB3 protein levels in PAOA/BSA-induced hepatocytes indicated by Western blots, β-ACTIN was used as internal control. **(G)** Representative ORO-staining images of mouse primary hepatocytes simulated by PAOA/BSA for 24 hours, scale bar = 50μm. **(H)** The mRNA levels of TRIB3 in PAOA/BSA-treated mouse primary hepatocytes, β-ACTIN was used as internal control, n = 3 per group. **(I)** TRIB3 protein levels in PAOA/BSA-induced mouse primary hepatocytes indicated by Western blots, β-ACTIN was used as internal control. \*p < 0.05, all data were shown as mean ± s.d.

**Abbreviations:** NC, Normal Chow diet; CDHFD, Choline-Deficient High-Fat Diet; H&E, Hematoxylin and Eosin; ORO, Oil Red O; BSA, Bovine Serum Albumin; PAOA, Palmitic Acid and Oleic Acid.

levels of IL-6, IL-1b, CCL2, and CXCL12 (Figure 6D). Our data suggest that the inhibition of TRIB3 in hepatocytes markedly ameliorates lipid accumulation and the inflammatory response induced by PAOA.

## Discussion

NAFLD is the most prevalent liver disease worldwide and is associated with a high risk of other metabolic syndromes, end-stage liver disease, and extrahepatic cardiovascular disease.<sup>23</sup> NASH, the terminal stage of NAFLD, is considered a component of metabolic syndrome, in which metabolic disorders occur in the fatty liver, resulting in systemic metabolic disorders.<sup>23</sup> Although much is still unknown about the pathogenesis of NAFLD, promising drug candidates



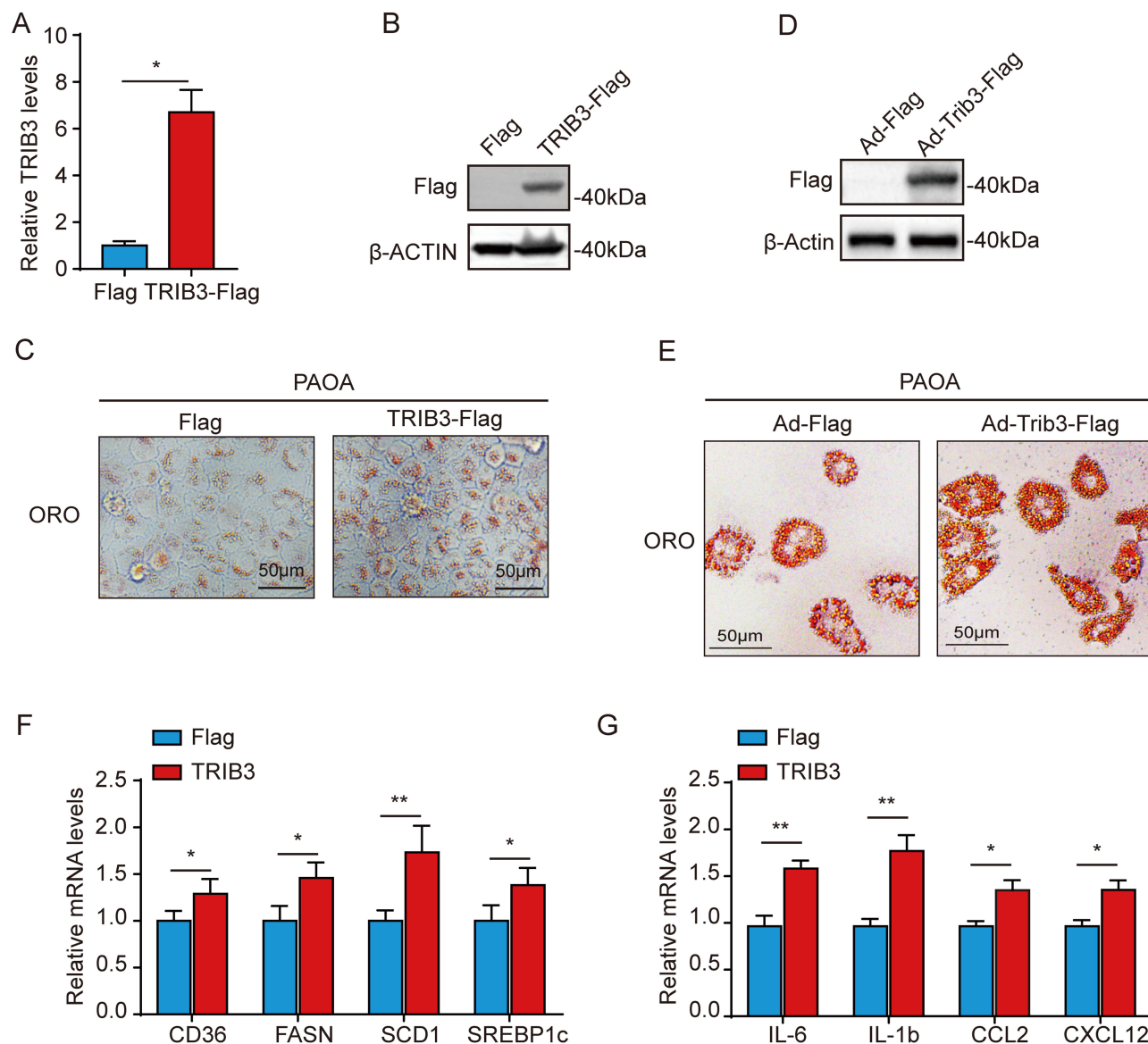


**Figure 5** TRIB3 overexpression aggravates PAOA-induced lipid accumulation and inflammation in hepatocytes. **(A)** qRT-PCR showed the relative mRNA expressions of TRIB3 in hepatocytes post pHAGE-Flag-TRIB3 plasmid transfection, pHAGE-Flag was used as control plasmid. β-ACTIN was used as internal control,  $n = 3$  per group. **(B)** Western blot analysis of TRIB3 protein expression in hepatocytes with TRIB3 gene overexpression by pHAGE-Flag vector; β-ACTIN was used as internal control. **(C)** Representative images of ORO-stained hepatocytes subjected to pHAGE-Flag-TRIB3 and pHAGE-Flag plasmids transfection stimulated by PAOA for 24 hours.  $n = 3$  independent experiments. Scale bar, 50 μm. **(D)** Western blot analysis of TRIB3 protein expression in mouse primary hepatocytes with mouse Trib3 gene overexpression by Ad-Flag vector; β-ACTIN was used as internal control. **(E)** Representative images of ORO-stained mouse primary hepatocytes infected with Ad-Trib3-Flag and Ad-Flag stimulated by PAOA for 24 hours.  $n = 3$  independent experiments. Scale bar, 50 μm. **(F)** qRT-PCR showed the relative mRNA expressions of fatty acid uptake gene (CD36) and lipid synthesis genes (FASN, SCD1 and SREBP1c) in the hepatocytes induced by PAOA. β-ACTIN was used as internal control,  $n = 5$  per group; **(G)** The relative genes expression associated with inflammation (IL-6, IL-1b, CCL2, CXCL12) were detected by qRT-PCR in hepatocytes administrated with PAOA for 12 hours. β-ACTIN was used as internal control,  $n = 5$  per group. \* $p < 0.05$ , \*\* $p < 0.01$ , all data were shown as mean  $\pm$  s.d.

**Abbreviations:** ORO, Oil Red O; PAOA, Palmitic Acid and Oleic Acid.

have failed in Phase II or III clinical trials over the past three years, further underscoring the urgent need to reveal the potential mechanisms for NASH.<sup>24</sup> Hepatocellular lipid deposition and the inflammatory response play important roles in the initiation of NAFLD and accompany the progression from NAFLD to NASH. To investigate the changes in hepatocyte gene expression and signaling pathways under steatohepatitis conditions and to identify hub genes, we screened and analyzed a microarray dataset from the Huh7 cell line induced by PAOA and compared it to control cells. The dataset GSE122660, we insight and analyzed, was produced by Breher-Esch et al in 2018 and contains 33 samples in 3 subdatasets, one of which we used for our present study.<sup>25</sup> Breher-Esch et al focused on the common and consistent

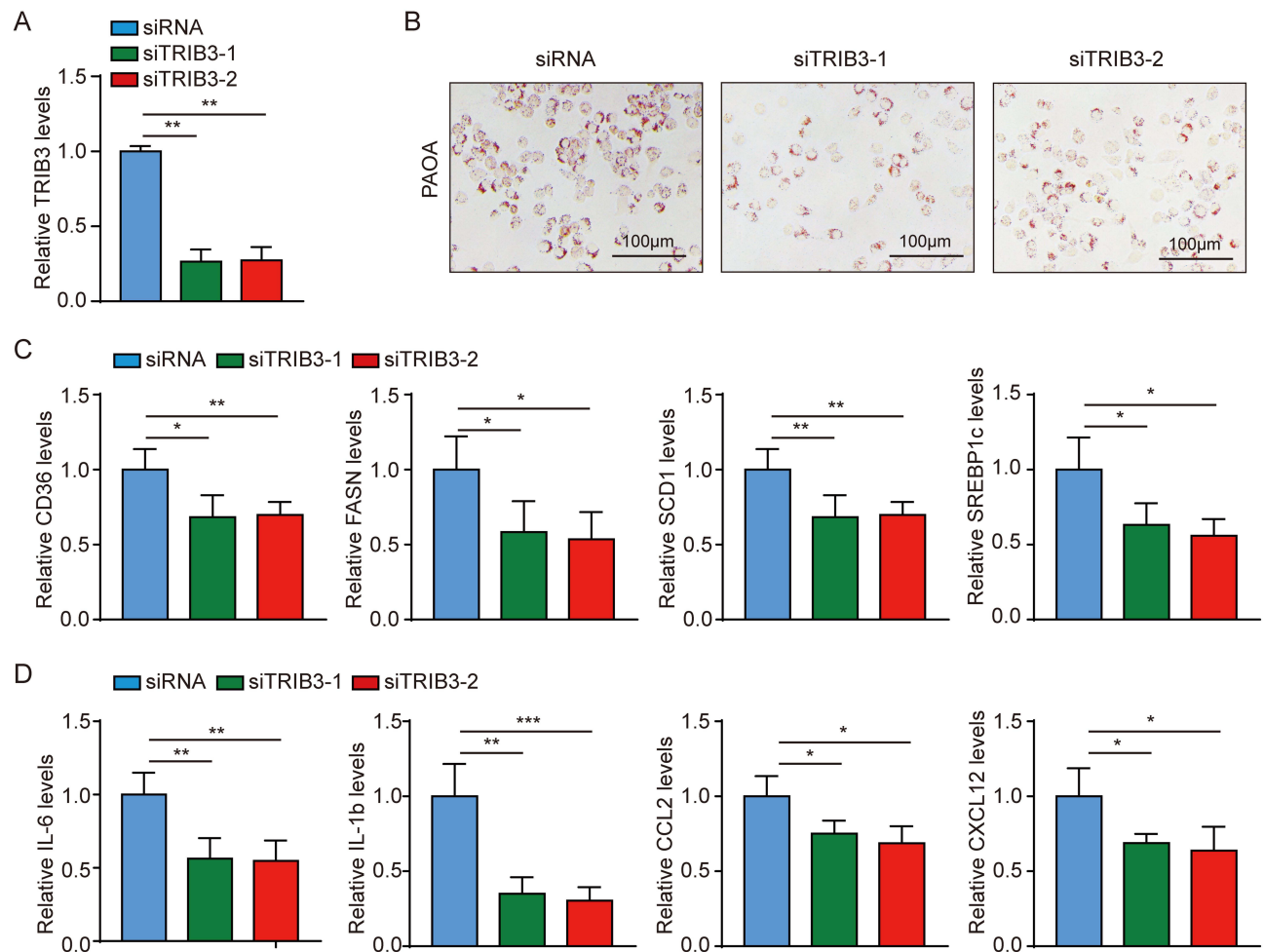


**Figure 6** Inhibition of TRIB3 expression ameliorates PAOA induced lipid accumulation and inflammation in hepatocytes. **(A)** qRT-PCR showed the relative mRNA expressions of TRIB3 in hepatocytes treated with siRNAs for 24 hours, respectively.  $\beta$ -ACTIN was used as internal control,  $n = 3$  per group. **(B)** Representative images of Oil Red O-stained hepatocytes transfected with siRNAs and stimulated by PAOA for 24 hours.  $n = 3$  independent experiments. Scale bar, 100  $\mu$ m. **(C)** qRT-PCR showed the relative mRNA expressions of fatty acid uptake gene (CD36) and lipid synthesis genes (FASN, SCD1 and SREBP1c) in the siRNAs-transfected hepatocytes induced by PAOA.  $\beta$ -ACTIN was used as internal control,  $n = 4$  per group. **(D)** qRT-PCR showed the expressions of inflammation related genes (IL-6, IL-1b, CCL2, CXCL12) in siRNAs-transfected hepatocytes administrated with PAOA for 12 hours.  $\beta$ -ACTIN was used as internal control,  $n = 4$  per group. \* $p < 0.05$ , \*\* $p < 0.01$ , \*\*\* $p < 0.001$ , all data were shown as mean  $\pm$  s.d.

**Abbreviations:** ORO, Oil Red O; PAOA, Palmitic Acid and Oleic Acid.

lipid droplet-associated gene changes in three different cell models in response to PAOA or TNF stimulation for 48 h or 72 h and revealed putative and established drug targets.<sup>25</sup> However, the systematic analysis of a single dataset and the derivation of hub genes were not the focus of the original authors, which is what we did in this study.

In the present study, we explored global genetic changes and attempted to identify hub genes in Huh7 cells after PAOA stimulation. We first identified 255 significant DEGs between PAOA-induced and control hepatocytes, and the top 20 upregulated genes were reported to be related to lipid metabolism and inflammatory response, including upregulated genes, such as *LAMP3*, *KLF4*, *SLC3A2*, *DDIT3*, and downregulated genes, such as *CCR6*, *PITX2*. Liao et al revealed that *LAMP3* was overexpressed in the liver tissues of NAFLD patients and high-fat diet and ob/ob mice compared to the matched control groups, and that *LAMP3* exacerbated hepatic lipid accumulation by activating the PI3K/Akt pathway.<sup>26</sup> *KLF4* is a native immune-related gene that regulates cellular inflammatory responses in the liver and extrahepatic tissue.<sup>27–29</sup> Hammerich et al found that mice with *Ccr6* knockout developed more severe fibrosis with strongly enhanced hepatic immune cell infiltration,<sup>30</sup> indicating that *CCR6* may play an anti-fibrotic role in NASH. Hu et al showed that *PITX2* suppression by deletion of the *PITX2* enhancer *ASE* aggravates diet-induced fatty liver disease.<sup>31</sup> Enrichment analysis of GO and KEGG pathways with DEGs showed that most of these DEGs were enriched in inflammation, lipid metabolism, and cell damage-related signaling pathways, and most of these signaling pathways have been identified in NAFLD.<sup>23,32,33</sup>

To identify the key regulatory and indicative molecules in the NAFLD process, PPI and hub gene analyses were performed. The data showed a total of 20 hub genes were highlighted, and 5 hub-gene with LogFC >1.5, including *GADD45A*, *ANXA1*, *VLDLR*, *TRIB3*, *DDIT3* and *PPP1R15A*. Previous study has revealed the endogenous ANXA1 plays a functional role in modulating hepatic inflammation and fibrogenesis during NASH progression,<sup>34</sup> and ANXA1 treatment prevents the evolution to fibrosis of experimental non-alcoholic steatohepatitis.<sup>35</sup> Tanaka et al showed that *GADD45A* plays a protective role in non-alcoholic steatohepatitis induced by methionine-and choline-deficient diet.<sup>36</sup> *DDIT3* is a gene that expresses CHOP protein and is considered a key gene in the endoplasmic reticulum. A large number of studies have supported the deterioration of NAFLD/NASH process by *DDIT3*/CHOP.<sup>32,37</sup> *VLDLR* belongs to the low-density lipoprotein receptor family and plays a role in triglyceride uptake. A previous study revealed that *VLDLR*-deficient mice exhibited decreased hepatic steatosis upon high-fat diet feeding.<sup>38</sup> Although recent studies have shown that *TRIB3* plays important roles in metabolism disorders,<sup>9,20</sup> the function of *TRIB3* in NAFLD has not been revealed yet.

Previous studies have suggested that *TRIB3* promotes insulin resistance<sup>39,40</sup> and inhibits adipocyte differentiation.<sup>41</sup> *Trib3* knockout mouse aortae exhibit reduced plaque development and improved plaque stability.<sup>42</sup> *TRIB3* upregulation has been associated with the development of a lean phenotype<sup>43</sup> and excessive *TRIB3* overexpression aggravates cholesterol accumulation in macrophages.<sup>44</sup> Yu et al showed that the NF- $\kappa$ B signaling pathway can be activated by *TRIB3* and triggers an inflammatory response.<sup>45</sup> Previous studies revealed that *TRIB3* is significantly upregulated in animal models of metabolic diseases including insulin resistance, obesity, and hyperglycemia.<sup>12,21,22</sup> In the present study, *TRIB3* was one of 138 upregulated DEGs, and we confirmed this conclusion by qRT-PCR and Western blotting in vitro and in vivo, suggesting that *TRIB3* plays a role in NAFLD. To further investigate the function of *TRIB3* in NAFLD in vitro, we established the *TRIB3*-overexpressed and -knockdown hepatocytes. Subsequent data suggested that *TRIB3* exacerbates steatohepatitis, as indicated by the detection of hepatocellular lipid droplets, steatohepatitis-related lipid metabolism, and inflammatory gene expression. Excessive lipid deposition in hepatocytes is a main trigger of liver inflammation, and together, these two factors contribute to the pathogenesis of the NAFLD/NASH process.<sup>46</sup> Inhibition of lipid synthesis and anti-inflammatory therapies have emerged as promising strategies for NAFLD/NASH treatment, and several drugs have been used in clinical trials.<sup>23</sup> In this study, overexpression of *TRIB3* simultaneously activated lipid synthesis and inflammatory response in hepatocytes, and *TRIB3* inhibition in hepatocytes markedly ameliorated lipid accumulation and inflammation. Therefore, targeting *TRIB3* might be a powerful new treatment strategy for NAFLD.

## Conclusion

In conclusion, our present study was based on the gene expression dataset obtained from the GEO database, we identified 255 DEGs and 20 hub genes in PAOA-induced hepatocytes compared to control cells, and the *TRIB3* was highlighted. We found that *TRIB3* is upregulated and exacerbates steatohepatitis in PAOA-induced hepatocytes by accelerating lipid accumulation and inflammation. Therefore, targeting *TRIB3* may be a potential pharmacological strategy for NAFLD treatment.

## Abbreviations

NAFLD, Non-alcoholic fatty liver disease; NASH, Non-alcoholic steatohepatitis; DEGs, differentially expressed genes; GO, Gene Ontology; KEGG, Kyoto encyclopedia of Genes and Genomes; PPI, Protein-protein interaction; *TRIB3*, tribbles pseudokinase 3; MetS, metabolic syndrome; CVDs, cardiovascular diseases; HCC, hepatocellular carcinoma; PAOA, palmitic acid and oleic acid.

## Data Sharing Statement

The datasets used and/or analyzed in the current study are available from the GEO dataset. software (<https://www.ncbi.nlm.nih.gov/geo/query/acc.cgi?acc=GSE122660>).

## Ethics Approval and Consent to Participate

This article does not include any studies involving human participants performed by any of the authors.

## Acknowledgment

This study was supported by the Wuhan NO.1 Hospital.

## Author Contributions

All authors made a significant contribution to the work reported, whether that is in the conception, study design, execution, acquisition of data, analysis and interpretation, or in all these areas; took part in drafting, revising or critically reviewing the article; gave final approval of the version to be published; have agreed on the journal to which the article has been submitted; and agree to be accountable for all aspects of the work.

## Funding

No funding was received for conducting this study.

## Disclosure

The authors have no relevant financial or non-financial interests to disclose.

## References

1. Pouwels S, Sakran N, Graham Y, et al. Non-alcoholic fatty liver disease (NAFLD): a review of pathophysiology, clinical management and effects of weight loss. *BMC Endocr Disord.* 2022;22(1):63. doi:10.1186/s12902-022-00980-1
2. Sun D, Yang X, Wu B, Zhang XJ, Li H, She ZG. Therapeutic potential of G protein-coupled receptors against nonalcoholic steatohepatitis. *Hepatology.* 2021;74(5):2831–2838. doi:10.1002/hep.31852
3. Friedman SL, Neuschwander-Tetri BA, Rinella M, Sanyal AJ. Mechanisms of NAFLD development and therapeutic strategies. *Nat Med.* 2018;24(7):908–922. doi:10.1038/s41591-018-0104-9
4. Zeigerer A. NAFLD - A rising metabolic disease. *Mol Metab.* 2021;50:101274. doi:10.1016/j.molmet.2021.101274
5. Targher G, Byrne CD, Tilg H. NAFLD and increased risk of cardiovascular disease: clinical associations, pathophysiological mechanisms and pharmacological implications. *Gut.* 2020;69(9):1691–1705. doi:10.1136/gutjnl-2020-320622
6. Huang DQ, El-Serag HB, Loomba R. Global epidemiology of NAFLD-related HCC: trends, predictions, risk factors and prevention. *Nat Rev Gastroenterol Hepatol.* 2021;18(4):223–238. doi:10.1038/s41575-020-00381-6
7. Raza S, Rajak S, Upadhyay A, Tewari A, Anthony Sinha R. Current treatment paradigms and emerging therapies for NAFLD/NASH. *Front Biosci.* 2021;26(2):206–237. doi:10.2741/4892
8. Grosshans J, Wieschaus E. A genetic link between morphogenesis and cell division during formation of the ventral furrow in *Drosophila*. *Cell.* 2000;101(5):523–531. doi:10.1016/S0092-8674(00)80862-4
9. Prudente S, Sesti G, Pandolfi A, Andreozzi F, Consoli A, Trischitta V. The mammalian tribbles homolog TRIB3, glucose homeostasis, and cardiovascular diseases. *Endocr Rev.* 2012;33(4):526–546. doi:10.1210/er.2011-1042
10. Tang Z, Chen H, Zhong D, et al. TRIB3 facilitates glioblastoma progression via restraining autophagy. *Aging.* 2020;12(24):25020–25034. doi:10.18632/aging.103969
11. Yokoyama T, Nakamura T. Tribbles in disease: signaling pathways important for cellular function and neoplastic transformation. *Cancer Sci.* 2011;102(6):1115–1122. doi:10.1111/j.1349-7006.2011.01914.x
12. Du K, Herzig S, Kulkarni RN, Montminy M. TRIB3: a tribbles homolog that inhibits Akt/PKB activation by insulin in liver. *Science.* 2003;300(5625):1574–1577. doi:10.1126/science.1079817
13. Wang L, Zhao W, Xia C, et al. TRIB3 mediates fibroblast activation and fibrosis through interaction with ATF4 in IPF. *Int J Mol Sci.* 2022;23(24):1.
14. Zhou H, Luo Y, Chen JH, et al. Knockdown of TRIB3 induces apoptosis in human lung adenocarcinoma cells through regulation of Notch 1 expression. *Mol Med Rep.* 2013;8(1):47–52. doi:10.3892/mmr.2013.1453
15. Lu Y, Li L, Chen L, Gao Y, Chen X, Cao Y. TRIB3 confers glioma cell stemness via interacting with beta-catenin. *Environ Toxicol.* 2020;35(6):697–706. doi:10.1002/tox.22905
16. Wennemers M, Bussink J, Scheijen B, et al. Tribbles homolog 3 denotes a poor prognosis in breast cancer and is involved in hypoxia response. *Breast Cancer Res.* 2011;13(4):R82. doi:10.1186/bcr2934
17. Shen P, Zhang TY, Wang SY. TRIB3 promotes oral squamous cell carcinoma cell proliferation by activating the AKT signaling pathway. *Exp Ther Med.* 2021;21(4):313. doi:10.3892/etm.2021.9744
18. Wang XJ, Li FF, Zhang YJ, Jiang M, Ren WH. TRIB3 promotes hepatocellular carcinoma growth and predicts poor prognosis. *Cancer Biomark.* 2020;29(3):307–315. doi:10.3233/CBM-201577
19. Miyoshi N, Ishii H, Mimori K, et al. Abnormal expression of TRIB3 in colorectal cancer: a novel marker for prognosis. *Br J Cancer.* 2009;101(10):1664–1670. doi:10.1038/sj.bjc.6605361
20. Lee SK, Park CY, Kim J, et al. TRIB3 is highly expressed in the adipose tissue of obese patients and is associated with insulin resistance. *J Clin Endocrinol Metab.* 2022;107(3):e1057–e1073. doi:10.1210/clinem/dgab780
21. Lima AF, Ropelle ER, Pauli JR, et al. Acute exercise reduces insulin resistance-induced TRIB3 expression and amelioration of the hepatic production of glucose in the liver of diabetic mice. *J Cell Physiol.* 2009;221(1):92–97. doi:10.1002/jcp.21833
22. Wang YG, Shi M, Wang T, et al. Signal transduction mechanism of TRIB3 in rats with non-alcoholic fatty liver disease. *World J Gastroenterol.* 2009;15(19):2329–2335. doi:10.3748/wjg.15.2329



23. Xu X, Poulsen KL, Wu L, et al. Targeted therapeutics and novel signaling pathways in non-alcohol-associated fatty liver/steatohepatitis (NAFL/NASH). *Signal Transduct Target Ther.* **2022**;7(1):287. doi:10.1038/s41392-022-01119-3
24. Tian R, Yang J, Wang X, et al. Honokiol acts as an AMPK complex agonist therapeutic in non-alcoholic fatty liver disease and metabolic syndrome. *Chin Med.* **2023**;18(1):30. doi:10.1186/s13020-023-00729-5
25. Breher-Esch S, Sahini N, Tricone A, Wallstab C, Borlak J. Genomics of lipid-laden human hepatocyte cultures enables drug target screening for the treatment of non-alcoholic fatty liver disease. *BMC Med Genomics.* **2018**;11(1):111. doi:10.1186/s12920-018-0438-7
26. Liao X, Song L, Zhang L, et al. LAMP3 regulates hepatic lipid metabolism through activating PI3K/Akt pathway. *Mol Cell Endocrinol.* **2018**;470:160–167. doi:10.1016/j.mce.2017.10.010
27. Chien Y, Huang CS, Lin HC, et al. Improvement of non-alcoholic steatohepatitis by hepatocyte-like cells generated from iPSCs with Oct4/Sox2/Klf4/Parp1. *Oncotarget.* **2018**;9(26):18594–18606. doi:10.18632/oncotarget.23603
28. Han YH, Kim HJ, Na H, et al. RORalpha induces KLF4-mediated M2 polarization in the liver macrophages that protect against nonalcoholic steatohepatitis. *Cell Rep.* **2017**;20(1):124–135. doi:10.1016/j.celrep.2017.06.017
29. Yang C, Xiao X, Huang L, et al. Role of Kruppel-like factor 4 in atherosclerosis. *Clin Chim Acta.* **2021**;512:135–141. doi:10.1016/j.cca.2020.11.002
30. Hammerich L, Bangen JM, Govaere O, et al. Chemokine receptor CCR6-dependent accumulation of gammadelta T cells in injured liver restricts hepatic inflammation and fibrosis. *Hepatology.* **2014**;59(2):630–642. doi:10.1002/hep.26697
31. Hu S, Mahadevan A, Elysee IF, et al. The asymmetric Pitx2 gene regulates gut muscular-lacteal development and protects against fatty liver disease. *Cell Rep.* **2021**;37(8):110030. doi:10.1016/j.celrep.2021.110030
32. Lebeaupin C, Vallee D, Hazari Y, Hetz C, Chevet E, Bailly-Maitre B. Endoplasmic reticulum stress signalling and the pathogenesis of non-alcoholic fatty liver disease. *J Hepatol.* **2018**;69(4):927–947. doi:10.1016/j.jhep.2018.06.008
33. Bessone F, Razori MV, Roma MG. Molecular pathways of nonalcoholic fatty liver disease development and progression. *Cell Mol Life Sci.* **2019**;76(1):99–128. doi:10.1007/s00018-018-2947-0
34. Locatelli I, Sutti S, Jindal A, et al. Endogenous annexin A1 is a novel protective determinant in nonalcoholic steatohepatitis in mice. *Hepatology.* **2014**;60(2):531–544. doi:10.1002/hep.27141
35. Gadipudi LL, Ramavath NN, Provera A, et al. Annexin A1 treatment prevents the evolution to fibrosis of experimental nonalcoholic steatohepatitis. *Clin Sci.* **2022**;136(9):643–656. doi:10.1042/CS20211122
36. Tanaka N, Takahashi S, Hu X, et al. Growth arrest and DNA damage-inducible 45alpha protects against nonalcoholic steatohepatitis induced by methionine- and choline-deficient diet. *Biochim Biophys Acta Mol Basis Dis.* **2017**;1863(12):3170–3182. doi:10.1016/j.bbdis.2017.08.017
37. Malhi H, Kaufman RJ. Endoplasmic reticulum stress in liver disease. *J Hepatol.* **2011**;54(4):795–809. doi:10.1016/j.jhep.2010.11.005
38. Jo H, Choe SS, Shin KC, et al. Endoplasmic reticulum stress induces hepatic steatosis via increased expression of the hepatic very low-density lipoprotein receptor. *Hepatology.* **2013**;57(4):1366–1377. doi:10.1002/hep.26126
39. Weismann D, Erion DM, Ignatova-Todorova I, et al. Knockdown of the gene encoding Drosophila tribbles homologue 3 (Trib3) improves insulin sensitivity through peroxisome proliferator-activated receptor-gamma (PPAR-gamma) activation in a rat model of insulin resistance. *Diabetologia.* **2011**;54(4):935–944. doi:10.1007/s00125-010-1984-5
40. Liu J, Wu X, Franklin JL, et al. Mammalian tribbles homolog 3 impairs insulin action in skeletal muscle: role in glucose-induced insulin resistance. *Am J Physiol Endocrinol Metab.* **2010**;298(3):E565–E576. doi:10.1152/ajpendo.00467.2009
41. Takahashi Y, Ohoka N, Hayashi H, Sato R. TRB3 suppresses adipocyte differentiation by negatively regulating ppargamma transcriptional activity. *J Lipid Res.* **2008**;49(4):880–892. doi:10.1194/jlr.M700545-JLR200
42. Martinez-Campesino L, Kocsy K, Canedo J, et al. Tribbles 3 deficiency promotes atherosclerotic fibrous cap thickening and macrophage-mediated extracellular matrix remodelling. *Front Cardiovasc Med.* **2022**;9:948461. doi:10.3389/fcvm.2022.948461
43. Qi L, Heredia JE, Altarejos JY, et al. TRB3 links the E3 ubiquitin ligase COP1 to lipid metabolism. *Science.* **2006**;312(5781):1763–1766. doi:10.1126/science.1123374
44. Stevenson D, Tian L, Fu Y, Zhang W, Ma E, Garvey WT. Tribbles homolog 3 promotes foam cell formation associated with decreased proinflammatory cytokine production in macrophages: evidence for reciprocal regulation of cholesterol uptake and inflammation. *Metab Syndr Relat Disord.* **2016**;14(1):7–15. doi:10.1089/met.2015.0037
45. Yu Y, Qiu L, Guo J, et al. TRIB3 mediates the expression of wnt5a and activation of nuclear factor-kappaB in Porphyromonas endodontalis lipopolysaccharide-treated osteoblasts. *Mol Oral Microbiol.* **2015**;30(4):295–306. doi:10.1111/omi.12094
46. Hirsova P, Ibrahim SH, Krishnan A, et al. Lipid-induced signaling causes release of inflammatory extracellular vesicles from hepatocytes. *Gastroenterology.* **2016**;150(4):956–967. doi:10.1053/j.gastro.2015.12.037

## Diabetes, Metabolic Syndrome and Obesity

### Publish your work in this journal

Diabetes, Metabolic Syndrome and Obesity is an international, peer-reviewed open-access journal committed to the rapid publication of the latest laboratory and clinical findings in the fields of diabetes, metabolic syndrome and obesity research. Original research, review, case reports, hypothesis formation, expert opinion and commentaries are all considered for publication. The manuscript management system is completely online and includes a very quick and fair peer-review system, which is all easy to use. Visit <http://www.dovepress.com/testimonials.php> to read real quotes from published authors.

Submit your manuscript here: <https://www.dovepress.com/diabetes-metabolic-syndrome-and-obesity-journal>

**Dovepress**  
Taylor & Francis Group